Dynamic Model of the Octopus Arm. II. Control of Reaching Movements

Yoram Yekutieli, Roni Sagiv-Zohar, Binyamin Hochner and Tamar Flash

J Neurophysiol 94:1459-1468, 2005. First published 13 April 2005; doi:10.1152/jn.00685.2004

J Neurophysiol 94: 1459–1468, 2005.
First published April 13, 2005; doi:10.1152/jn.00685.2004.

Dynamic Model of the Octopus Arm. II. Control of Reaching Movements

Yoram Yekutieli,[1,2] Roni Sagiv-Zohar,[1] Binyamin Hochner,[1,2] and Tamar Flash[3]

[1]*Department of Neurobiology and* [2]*Interdisciplinary Center for Neural Computation, Hebrew University, Jerusalem; and* [3]*Department of Computer Science and Applied Mathematics, Weizmann Institute of Science, Rehovot, Israel*

Submitted 6 July 2004; accepted in final form 2 March 2005

Yekutieli, Yoram, Roni Sagiv-Zohar, Binyamin Hochner, and Tamar Flash. Dynamic model of the octopus arm II. Control of reaching movements. *J Neurophysiol* 94: 1459–1468, 2005. First published April 13, 2005; doi:10.1152/jn.00685.2004. The dynamic model of the octopus arm described in the first paper of this 2-part series was used here to investigate the neural strategies used for controlling the reaching movements of the octopus arm. These are stereotypical extension movements used to reach toward an object. In the dynamic model, sending a simple propagating neural activation signal to contract all muscles along the arm produced an arm extension with kinematic properties similar to those of natural movements. Control of only 2 parameters fully specified the extension movement: the *amplitude* of the activation signal (leading to the generation of muscle force) and the *activation traveling time* (the time the activation wave takes to travel along the arm). We found that the same kinematics could be achieved by applying activation signals with different activation amplitudes all exceeding some minimal level. This suggests that the octopus arm could use minimal amplitudes of activation to generate the minimal muscle forces required for the production of the desired kinematics. Larger-amplitude signals would generate larger forces that increase the arm's stability against perturbations without changing the kinematic characteristics. The robustness of this phenomenon was demonstrated by examining activation signals with either a constant or a bell-shaped velocity profile. Our modeling suggests that the octopus arm biomechanics may allow independent control of kinematics and resistance to perturbation during arm extension movements.

INTRODUCTION

The octopus arm—a unique tool that combines strength and flexibility—shortens, elongates, bends, and twists at any point along the arm. It can perform a large variety of motor tasks such as dexterous manipulation of small objects, swiftly seizing prey, building a shelter (Wells 1978; Wells and Wells 1957), and opening a jar (Fiorito et al. 1990). Lacking any rigid skeletal support and using muscles to create a dynamic skeleton, the arm can be described as a *muscular hydrostat* (Kier and Smith 1985). In the language of robotics, the octopus arm is a hyperredundant manipulator; i.e., it has many more than the minimal number of degrees of freedom (DOFs) required to fully specify the position and orientation of an object in space (Chirikjian and Burdick 1994). Having a large number of DOFs poses a considerable challenge to the motor control system (Chirikjian and Burdick 1994; Hollerbach 1990).

The octopus extends its arms by creating a bend, usually near the base of the arm (but it can be formed almost anywhere along the arm), which is then propagated along the arm to the tip (Gutfreund et al. 1996). The arm remains relatively straight proximally to the bend, and the bend is always curved dorsally [Fig. 5*A* in the first paper of this 2-part series (Yekutieli et al. 2005), hereafter referred to as "paper I"]. Electromyograms (EMG) recorded from the arm muscles showed that this traveling bend is associated with a propagating wave of muscle activation (Gutfreund et al. 1998). In addition, EMG activity levels during the initial phase of the reaching movement correlate positively with the maximal tangential velocity of the bend point that develops afterward. This suggests that reaching movements are largely controlled by a feed-forward motor command evoking forward propagation of a wave of muscle stiffening that pushes the bend forward. Because stimulating the axial nerve cord of a denervated octopus arm evoked extension movements with kinematics similar to those of natural movements, the ability to produce an extension movement is embedded within the arm itself (Sumbre et al. 2001).

Gutfreund et al. (1996) suggested that this stereotypical movement solves the inverse kinematics and inverse dynamics problems associated with the control of movements involving many DOFs. The octopus achieves effective control by using only a small number of control variables, which may lead to coupling between different DOFs. In the case of directed reaching movements, the octopus appears to control only 2 angles to orient the base of the arm and another variable to control the speed of propagation of the bend along the arm.

METHODS

To test the suggestion advanced by Gutfreund et al. and to explore this unique control system, we have developed a dynamic model of the octopus arm, described fully in paper I. Briefly, the model arm consists of 20 segments with constant volume (paper I, Fig. 1). The total mass of the arm is divided among point masses located at the vertices of the segments. These masses are connected by springs representing the longitudinal and transverse muscles. The force–length properties of the muscles (Fig. 1*A*) are based on our experimental measurements of the *Octopus vulgaris* arm muscles (H. Matzner and B. Hochner, unpublished data) and on published results from muscles in related animals (see details in paper I). The relaxed length[1] of the muscles was $0.8l_0^m$, where l_0^m is the length at which the active muscle force is maximal (see paper I). The actual force produced by each muscle of a segment in the model was calculated using the dimensions of the segment.

[1] *Relaxed length* is the characteristic length of a muscle that is neither activated nor subjected to external forces. A muscle set to this length can produce force only if it is activated. However, for greater lengths, a resistive force can be detected without activation (paper I, Fig 6A).

Address for reprint requests and other correspondence: T. Flash, The Faculty of Mathematics and Computer Science, The Weizmann Institute of Science, POB 26, Rehovot 76100, Israel (E-mail: tamar.flash@weizmann.ac.il).

The costs of publication of this article were defrayed in part by the payment of page charges. The article must therefore be hereby marked "*advertisement*" in accordance with 18 U.S.C. Section 1734 solely to indicate this fact.

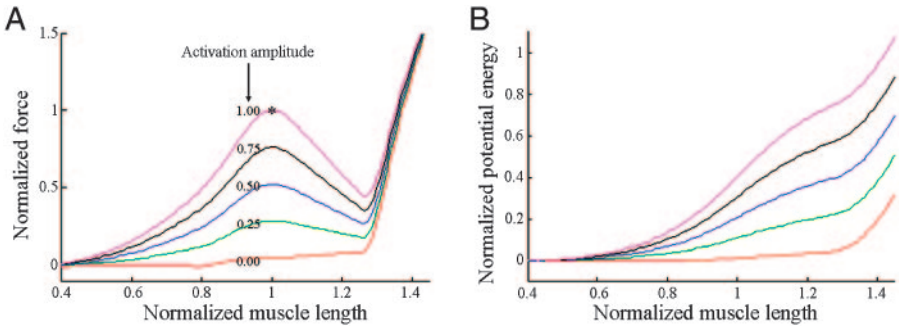

FIG. 1. *A*: force–length relationship of the muscle model. Each curve is the sum of the active and passive force–length properties of the muscle. Asterisk marks the peak of active force at maximal muscle activation. Force and muscle length values are normalized by the force and length at this point (muscle length is l_0^m,). Curves show different contributions of the active force ranging from no active force (zero activation in the model, *bottom curve*) to maximal active force (maximal activation, *top curve*). *B*: potential energy stored in the muscles vs. muscle length. Each curve is the numerical integral of the matching force curve in *A*. Potential energy is a monotonically increasing function of muscle length.

The input to the model was a simple activation wave traveling along the arm at a constant speed (paper I, Fig. 5) and activating all muscles to exactly the same degree. This pushed a bend that traveled along the arm while keeping the muscles activated. The model replicates extension movements with similar appearance and kinematics to those generated by the octopus (paper I, Figs. 6 and 8). Here we use this model to study how the commands to the muscles determine the kinematics of the extension movement and its resistance to external forces.

Extensions were simulated, varying both the amplitude of the muscle activation command and the time taken by the signal to travel along the arm. Each simulation produced a curve varying over time that gave the shape of the modeled arm. The position of the point of maximal curvature along the arm (the *bend point*) was marked in time and its tangential velocity profile[2] was calculated. We also simulated the reaching movement in the presence of a perturbing force—either a constant force field directed downward (an increased gravitational field) or upward. As in other simulations of extension movements, we analyzed the kinematics of the movements, focusing on the bend point paths and velocities.

RESULTS

The simulated reaching movement and its mechanism

When an octopus reaches toward a target, its arm extends and straightens. Here we show how the force–length properties of the muscles and the constant volume of each segment in our dynamic model lead to the arm straightening. First, we investigate the behavior of a single segment and show that equal activation of all the muscles in a segment cause it to become rectangular. We then describe how the simulated arm straightens as its individual segments assume this rectangular shape.

SHAPE CHANGES OF A SINGLE SEGMENT. If all 4 muscles of a segment are at their relaxed length ($0.8l_0^m$), then because of the constant area constraint,[3] the *relaxed shape* of the segment (i.e., when no active forces are present) is approximately rectangular.[4]

The dynamics of shape changes of a segment is depicted graphically in Fig. 2. The figure shows the difference in force production between a longitudinal and a transverse muscle in a rectangular segment as a function of the length of these 2 muscles, with values based on the force–length properties of the muscles (Fig. 1*A*, *top curve*). Here we assume that the 2 muscles are independent, have identical properties,[5] and are

[5] The balance of forces between the longitudinal and transverse muscle groups is based on the assumption that the arm's muscle fibers are homogenous and evenly distributed throughout the arm (paper I) and on the findings that functionally antagonistic longitudinal and transverse muscle fibers show no differences in membrane properties and mode of innervation (Matzner et al. 2000).

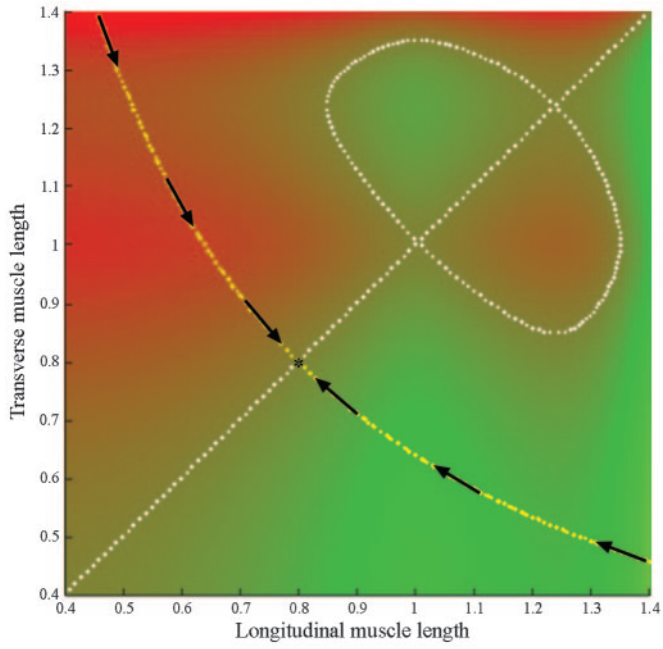

FIG. 2. Relation between the forces generated by the longitudinal and the transverse muscles of one rectangular segment at maximal muscle activation. Background color denotes the difference in force between the muscles as a function of muscle length: red, the transverse muscles generate a larger force; green, the longitudinal muscles generate a larger force. White dots: the transverse and longitudinal muscles generate the same force (based on the force–length relations in Fig. 1). Yellow: the relation between the lengths of the transverse and longitudinal muscles attributed to the constant area (volume) constraint. Relaxed length of each muscle is 0.8 l_0^m so the area is 0.64 $(l_0^m)^2$, which gives the relation $y = 0.64/x$ (yellow curve). Arrows on this curve show the direction of the length changes along it. In the upper part the transverse muscles have larger force so they contract and are able to stretch the longitudinal muscles. In the lower part, the opposite happens. Eventually the transverse and longitudinal muscles converge to their relaxed length (asterisk) and, with them, the segment moves to its relaxed shape.

[2] Tangential velocity is the velocity in the direction of movement and is calculated from the coordinates of the bend point according to: $V_{tan} = \sqrt{\dot{x}^2 + \dot{y}^2}$

[3] We can consider areas instead of volumes because the depth of each segment in the model does not change in time so the constant volume constraint of muscular hydrostats is kept. See paper I for the detailed description of the model.

[4] The relaxed length of each muscle is 0.8 l_0^m. If we assume, for a given segment, an equal l_0^m for all four muscles and an area of $(0.8\ l_0^m)^2$ then the shape of this segment must be a square. However, in its relaxed state, the arm tapers from base to the tip, making the proximal transverse muscle in each segment a little longer than the distal one. The two longitudinal muscles have the same length, which is generally different from the length of the transverse muscles. As a result, the actual shape of a relaxed segment is a trapezoid. When normalizing the lengths by l_0^m, the normalized shape is a square.

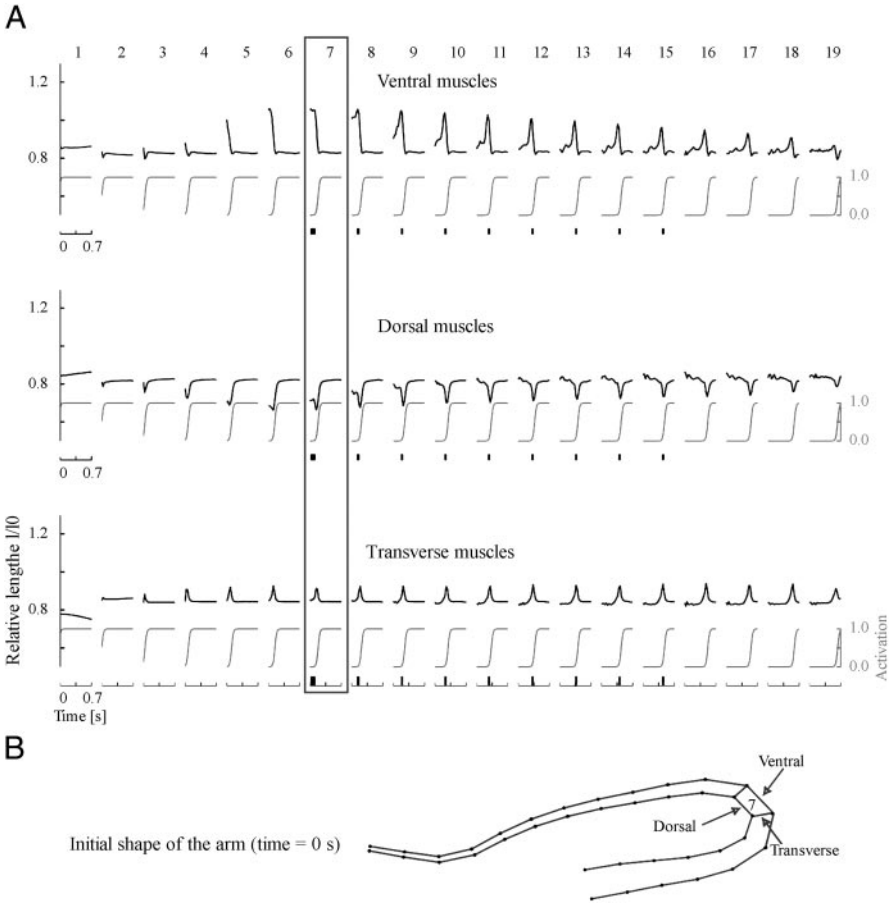

FIG. 3. *A*: muscle length, activation, and bend point occurrence against time in all segments of an arm during a simulated movement. Each column describes 3 muscles within a segment; segment number is shown at the *top*. Different rows show the ventral, dorsal, and transverse muscles. For each muscle, the *top curve* (black) shows muscle length vs. time. Curve below (light gray) is the magnitude of activation of the muscle vs. time and is identical for the 4 muscles of a segment. Small bars show the time at which the bend point was located at the segment (bend time). Note that the bend time is identical by definition for the 3 muscles of the same segment. Abscissa of all graphs is a time axis, range 0–0.7 s. Ordinate of all *top curves* (black) is normalized length (muscle length divided by l_0^m). 0.8 l_0^m is the relaxed length of each muscle. Ordinate of all *bottom curves* (light gray) shows activation (from 0 to 1, shown on the *right*). Vertical rectangle marks segment No. 7 where the bend time is at $t = 0$. *B*: initial shape of the arm (at $t = 0$). Segment No. 7 and its 3 muscles are marked.

maximally activated. The 2 muscles generate equal force along the diagonal (where they have the same length) and for other combinations of lengths (all depicted by the white dots) that arise from the nonmonotonic properties of the muscles' force–length curves.

Now, because of the constant area constraint, the lengths of the 2 muscles are dependent on each other, as depicted by the yellow curve in Fig. 2. As long as the longitudinal muscle has a larger force, it will contract, causing the transverse muscle to stretch. The only point of equal force that also keeps the area constant is the crossing point of the diagonal and the yellow curve, which is at the same length as the relaxed length of all muscles. Therefore the segment is bound to assume its relaxed shape.

For the simple case of a rectangular segment with linear muscles, we show analytically that the relaxed shape achieves a minimal potential energy (see APPENDIX A). In APPENDIX B we show that for a general quadrilateral of constant area, the shape with minimal potential energy is the relaxed shape, making this the preferred shape.

MUSCLE LENGTH CHANGES DURING THE SIMULATED MOVEMENT. Figure 3 describes in detail the changes in muscle length and activation during a typical simulated reaching movement. In the model structure, each segment is bounded by 2 longitudinal muscles (one dorsal and one ventral) and 2 transverse muscles (one proximal and one distal) (see paper I, Fig. 1). The transverse muscles are shared by adjacent segments and, to avoid duplications, we use the convention that each segment has only one transverse muscle with the same index. Figure 3*A* shows the changes in length as a function of time for all muscles in the model arm. All 3 muscles of a segment receive equal activation, depicted as a function of time by the light gray curves.

The initial shape of the arm at $t = 0$ is shown in Fig. 3*B*, and here the bend point (the point of maximal curvature) appears in segment 7. The ventral muscle of this segment is extended beyond its relaxed length because it lies at the outer contour of the arm. From Fig. 3*A* (*top row*, *7th column*), we see that the initial length ($t = 0$) of this muscle is $1.1l_0^m$. The dorsal muscle, on the other hand, at the inner side of the bent arm, is much shorter (*middle row*, *7th column*), about $0.7l_0^m$. As time advances, the length of the ventral muscle fluctuates slightly and decreases to $0.8l_0^m$. The length of the dorsal muscle fluctuates too, and then increases with the same time course as the ventral muscle to $0.8l_0^m$.

All other muscles (including the transverse muscles) also reach the length $0.8l_0^m$ during the simulation. Just below the force–length curve of each muscle (black curve), the light gray curve shows the activation function versus time for that muscle. For all muscles, whenever the activation reaches its maximal value of 1.0, the muscle length approaches $0.8l_0^m$, which is also the relaxed length of each muscle.

THE MECHANISM OF ARM EXTENSION. In the simulated reaching movements, the initial arm shape (paper I, Fig. 7*A*, 0 ms) is the typical shape of the octopus arm just before extension. An activation signal travels along the arm, contracting the muscles and pushing the bend distally. The path of the bend point (paper I, Fig. 7*B*) is an almost straight line, differing slightly from the typical slightly curved bend paths of natural extension

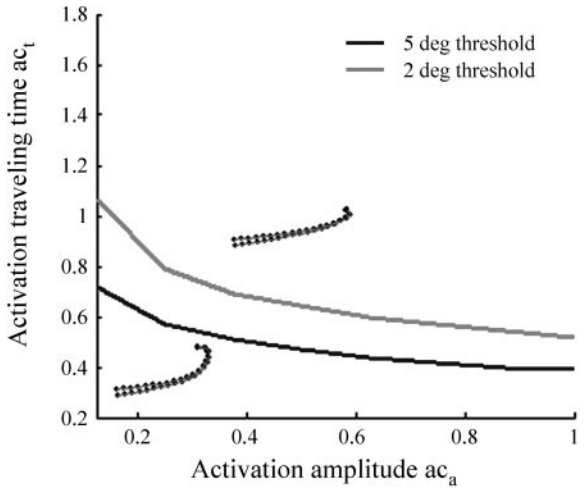

FIG. 4. Relation between activation traveling time (ac_t) and activation amplitude (ac_a) as revealed by the shape of the arm. Combinations of ac_t and ac_a on the gray curve produce a straight arm toward the end of the simulated extension (like the upper arm shape) with average local angle between arm segments of 2°. Combinations of ac_t and ac_a on the black curve produce the arm toward the end of the simulated extension (like the lower arm shape) with a 5° average local angle between arm segments. Parameter space is thus divided into 2 domains: the area above and to the *right* of the gray curve, where any combination of ac_t and ac_a produces a straight arm, and the area below and to the *left* of the gray curve, where the further from the curve the parameters are chosen, the more curved the arm is.

movements (straight paths have also been observed) (Gutfreund et al. 1998). The tangential velocity profile of the bend point has a sharp acceleration phase and a moderate decline (paper I, Fig. 7*C*). This profile was compared with the natural extension movement in paper I.

The arm extension mechanism is based on the behavior of the single segment as described above. The proximal segments have an initial shape close to their relaxed shape. Equally activating their muscles transforms them to their relaxed shape, making the base of the arm straight. Thus the proximal part of the arm that is subjected to constant activation is already straightened and resists shape changes. As seen in paper I, Figs. 6 and 7, the bend moves distally along the arm preceding the activation front, as a result of the transfer of forces from the activated segments to adjacent nonactivated ones.

Control of the reaching movement

The problem of controlling a reaching movement is how to activate muscles so that the arm reaches a desired point in space at a specific time. In analyzing the motor control of the octopus arm, we limit our study to the simple muscle command described in paper I, a wave of muscle activation that travels along the arm at a constant velocity and equally activates all the muscles it reaches. These muscles remain activated until the end of the extension movement. Here we consider 2 parameters that characterize this signal: the activation amplitude ac_a and the activation traveling time ac_t. These parameters may control the timing of the movement and the position that the tip of the arm reaches, as manifested in the shape of the tangential velocity profiles.

We ask the following questions: What is the minimal activation amplitude that still preserves the kinematic features of a reaching movement? What happens when activation amplitude is even lower? Is there a relation between the minimal activation amplitude and the activation traveling time?

THE STRAIGHTNESS OF THE ARM. During natural and evoked reaching movements by the octopus, the part of the arm between the base and the bend forms an almost straight line (paper I, Fig. 6, *A* and *B*). We used this feature to define a qualitative measure of the simulated reaching movements. To measure straightness, we took the averaged curvature along the already activated part of the arm, using the local angle between any 2 ventral muscles along the arm as a discrete approximation to curvature. An appropriate reaching movement was signified by an averaged local angle of 2° or less measured at only one point in time near the end of the movement (Fig. 4).

We then searched for combinations of ac_a and ac_t that produced straight arm shapes toward the end of the simulated extension movements. The results in parameter space are depicted by the gray curve in Fig. 4. For comparison, the black curve in Fig. 4 represents the combinations of these two parameters that produced a curved arm shape (with 5° as an average value of the local angles). Any combination of ac_a and ac_t in the *top right* area of the parameter space results in a straight arm. Combinations from the *bottom left* area produce curved arm shapes. We shall relate these results to efficiency and control of arm movements.

CHANGING ACTIVATION TRAVELING TIME AND FIXING ACTIVATION AMPLITUDE. Figure 5 shows that, when fixing activation amplitude (ac_a) and changing activation traveling time (ac_t), there are large changes in the maximum velocity and small changes in the time to peak. The longer the activation traveling time is, the lower the velocity peak and the later the time to peak. Note that the maximal velocity of the bend point is almost the same as the constant velocity of the activation signal. This means that for the movements in Fig. 5, the activation signal caused the muscles to generate enough force to accelerate the bend until it traveled at almost the same speed as the neural command signal.

CHANGING ACTIVATION AMPLITUDE AND FIXING ACTIVATION TRAVELING TIME. Figure 6*A* shows a group of 6 velocity profiles of movements with different activation amplitudes (ac_a) but the same activation traveling time (ac_t). The velocity profiles are very similar. That is, one can create a reaching movement with specific properties (i.e., time and amplitude of the maximal tangential velocity) by choosing from a range of activation amplitudes.

How general is this independence of the kinematics from the activation amplitude? The movements, whose velocity profiles are seen in Fig. 6*A*, like other movements already described, were simulated using activation signals with constant velocity profiles. In paper I, we also examined movements driven by activation signals with variable, bell-shaped velocity profiles. The velocity profiles of these movements are shown in Fig. 6*C*. The shape of their velocity profiles differs from those in Fig. 6*A* but, again, the use of the same activation traveling time with different activation amplitudes produces very similar velocity profiles.

Notice that the relation between ac_t, ac_a, and the kinematics for movements with constant velocity for the activation signal, as depicted by the 2° curve in Fig. 6*B*, is similar in form but different in value from the relation for movements driven by activation signals with bell-shaped velocity profiles (Fig. 6*D*). The latter required longer activation traveling times for the same activation amplitudes to straighten the arm.

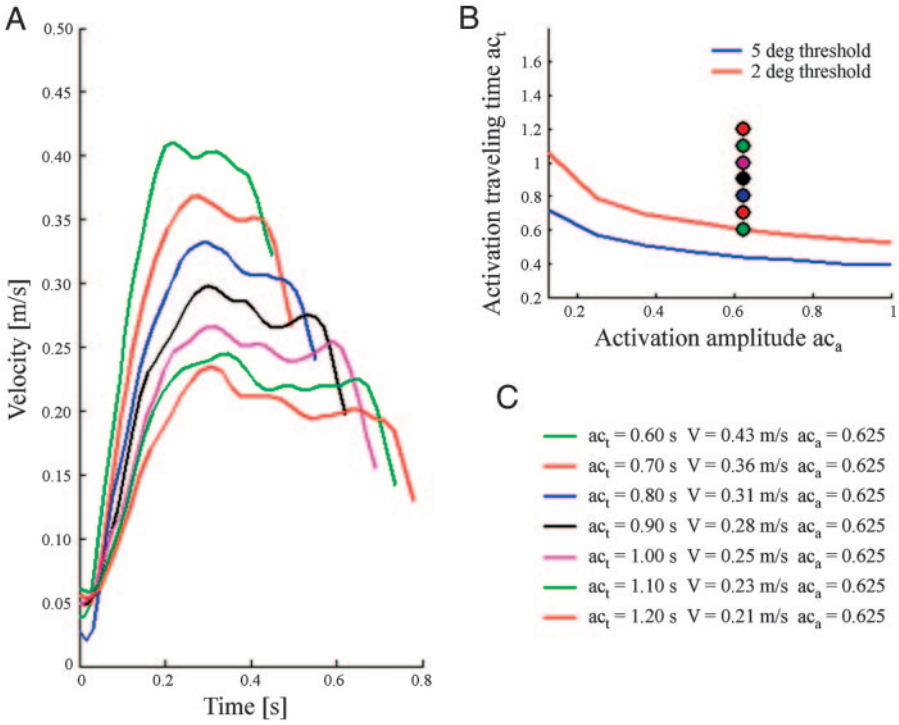

FIG. 5. *A*: 7 velocity profiles of simulated reaching movements differing in activation traveling time ac_t for the same activation amplitude, ac_a = 0.625. Combination of ac_t and ac_a for each movement in *A* is shown as circles in *B*, using the same colors. *C*: ac_t, *V*, and ac_a values for each movement. *V*, the constant velocity at which the activation wave travels along the arm, depends on ac_t and the length of the arm.

MINIMUM FORCE CONTROL. Values of the 2 control parameters ac_a and ac_t above and to the right of the light gray curve in Figs. 4 and 6 or the red curve (2° threshold) in Fig. 5 represent combinations of these parameters that produce different reaching movements, all of which comply with the criterion of arm straightness. Any increase in ac_t from any combination on the 2° curve can be used to control the maximal velocity of the bend point (Fig. 5*A*), but a reaching movement with the same velocity profile can be achieved by different forces (Fig. 6*B*). Thus the combination with minimal force that still produces an acceptable reaching movement with this velocity profile lies on the 2° curve.

Because there is a direct connection in our model between activation amplitude and muscle force we term the 2° curve the *minimum force curve*, suggesting the presence of a possible minimum force control scheme, which uses the minimal acti-

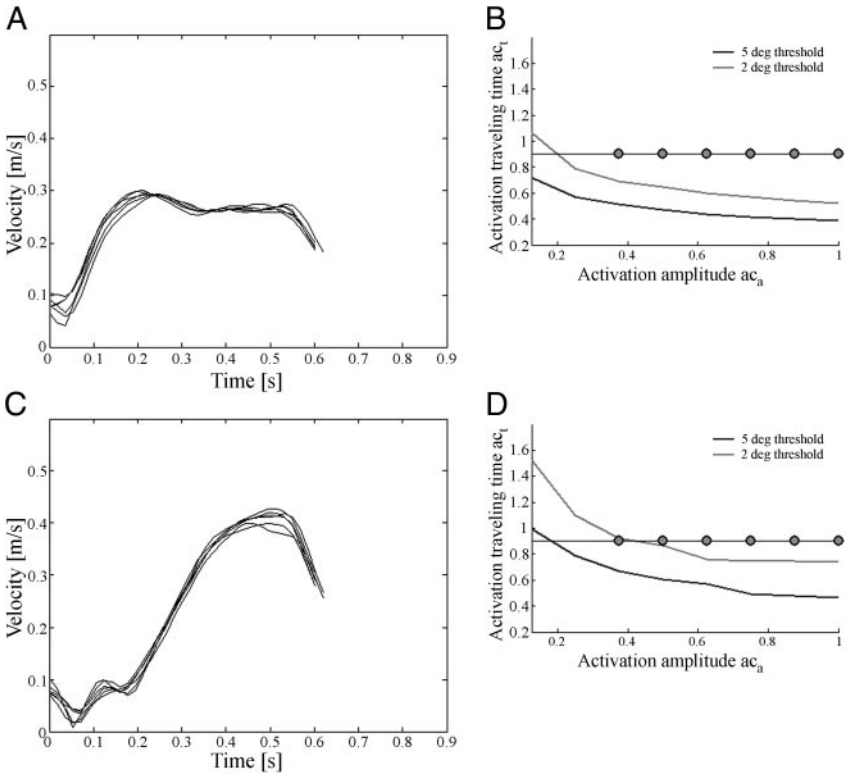

FIG. 6. *A*: group of 6 velocity profiles of simulated reaching movements all for muscle activation signals with the same constant velocity, *V* = 0.28 m/s. Their activation traveling time ac_t = 0.9 s, and activation amplitudes ac_a vary from 0.375 to 1.0. Combination of ac_t and ac_a for each movement in *A* is shown as circles in *B*. All movements are chosen with combinations of ac_a and ac_t above the 2° curve. *C*: as in *A*, but the activation signals have bell-shaped velocity profiles. Activation traveling times ac_t = 0.9 s as in *A*, so averaged signal velocity is also 0.28 m/s. Activation amplitudes ac_a vary from 0.375 to 1.0. Combination of ac_t and ac_a for each movement in *C* is given by the circles in *D*. All movements are chosen with combinations of ac_a and ac_t on or above the 2° curve.

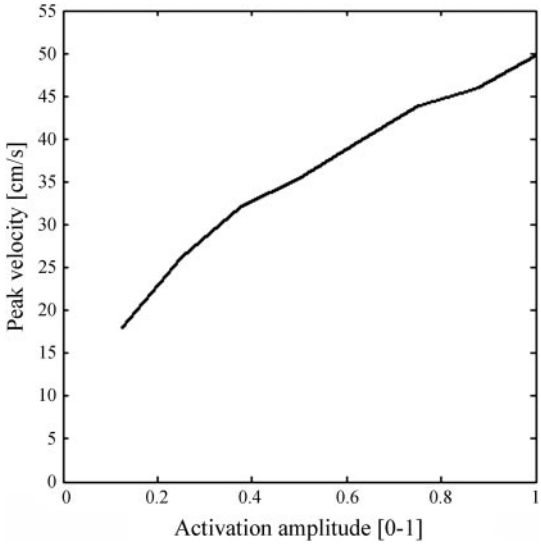

FIG. 7. Relation between peak velocity (the maximal tangential velocity of the bend point) and activation amplitude for simulations whose activation traveling times and activation amplitudes were coupled according to the minimal force curve. A similar relation between the peak velocity of the bend and the integrated EMG was found experimentally by Gutfreund et al. (1998).

vation (thus forces) needed to produce a desired kinematics (see DISCUSSION).

THE RELATION BETWEEN BEND VELOCITY AND ACTIVATION AMPLITUDE. Gutfreund et al. (1998) demonstrated a linear relation between integrated EMG and the peak velocity of the bend point. We examined the relation between the bend's peak velocity and the activation amplitude (ac_a) using several simulated arm extensions whose activation traveling times and activation amplitudes were coupled according to the minimal force curve. The results (Fig. 7) show a slightly curved positive relation between the two variables, very similar to the experimental results of Gutfreund et al. (1998).

Open arm extension movements

The simulated arm straightens out as in natural movements if the force generated is high enough and if this force has enough time to act (Fig. 4). When the force is too low, the activation wave passes the bend point and no longer pushes it. This causes the distal part of the arm to be extended, not by propagating the bend, but by a uniform reduction of arm curvature. If this phenomenon is taken to the extreme—using a very short activation traveling time—no muscle force (in the physiological range) would be high enough to push the bend forward and the whole arm would open uniformly in a movement that we term "open arm extension" (Fig. 8*A*).

This type of arm movement can be induced in a denervated octopus arm preparation (Fig. 8*B*) by intense stimulation that apparently overrides the arm extension motor program. The neural response to this stimulus appears to propagate quickly along the axial nerve cord (about 3.0 m/s, unpublished data) to cause an almost instantaneous activation of the nearly 40,000 motoneurons (Young 1965), which then cause all the arm's musculature to contract almost simultaneously (G. Sumbre and B. Hochner, unpublished observations).

Resisting perturbing forces

Because large forces within the arm do not change the kinematics of the simulated extension movements (see Fig. 6), at least from the energetic perspective, it is more efficient to choose the minimal muscle force according to the minimal force curve. However, using higher forces could stabilize the arm against perturbing forces.

We checked the kinematics of simulated movements subjected to an external force, either a simple constant force field pointing downward (increased gravitational field), the reverse, or no perturbing force at all. In each case we simulated the extension movement with either a low ac_a of 0.125 (to give low muscle forces) or a high ac_a of 1.0 (resulting in high muscle forces) and examined the path of the bend point and the final shape of the arm.

Figure 9 shows little difference between simulations with low and high arm force when no external force was applied. Applying an upward or downward force field affected all movements. However, simulations using high forces within the arm showed a higher resistance to the perturbing force.

DISCUSSION

Two possible mechanisms of bend propagation

Kier and Smith (1985) suggested that a bend in a muscular hydrostat can be created when the longitudinal muscles of one side of the arm contract together with the transverse muscles. The bend may be formed either by a unilateral decrease in length while keeping the diameter constant or by decreasing

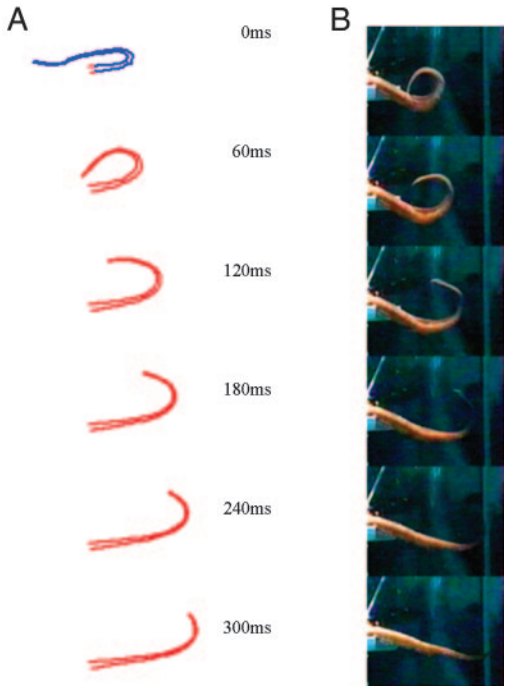

FIG. 8. *A*: sequence showing the simulated "opening arm extension." Red represents the arm segments that are fully activated, blue the nonactivated segments. Activation traveling time was very short so that all the arm muscles were activated just after the beginning of the simulation; the result of such activation is a uniform reduction of arm curvature, i.e., only minor bend propagation can be seen. *B*: video sequence showing an opening arm extension in a denervated arm preparation after a high-amplitude stimulus to the axial nerve cord.

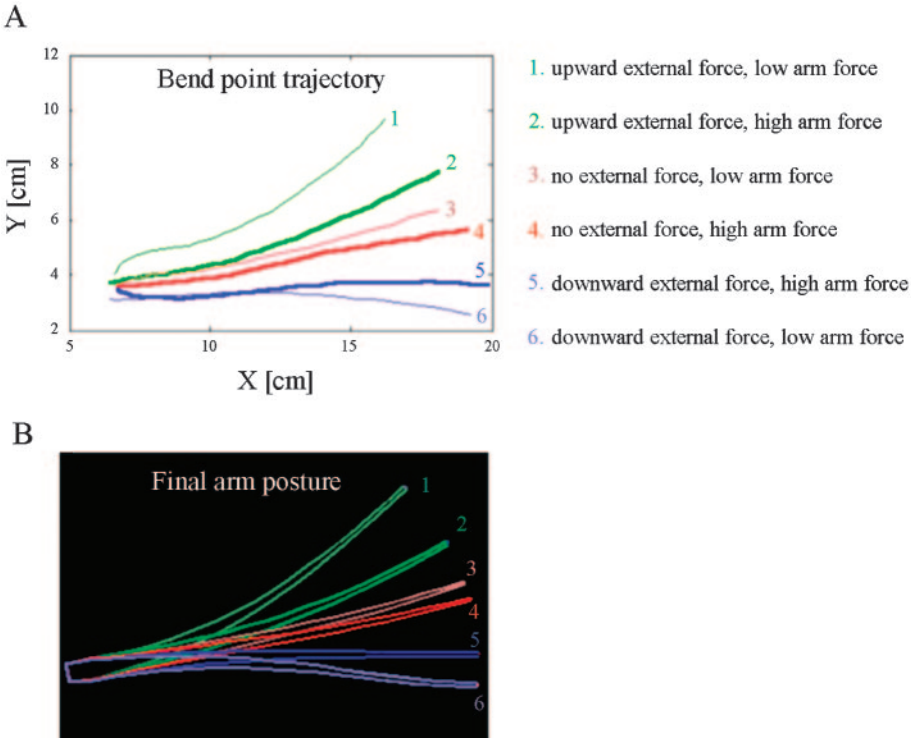

FIG. 9. Simulations of reaching movements with low or high muscle activation (causing low or high force within the arm) were subjected to different external forces: an upward pulling force, a downward pulling force, or no external force. *A*: bend point trajectory of the 6 simulated reaching movements. *B*: final arm posture of the 6 simulated reaching movements.

the diameter while keeping the length of the one side constant. This pattern of muscle activation can then be propagated along the arm creating an extension movement.

However, Gutfreund et al. (1998) found no evidence for differential activation of dorsal and ventral muscle groups during reaching movements. Instead, the EMG signal had the same shape and amplitude at recording electrodes positioned at different orientations across the arm. They therefore proposed a different mechanism for bend propagation: a stiffening wave caused by a symmetrical muscle activation pattern that propagates along the arm, propelling an existing passive bend. Although there was no conclusive evidence to support this idea, it is an attractive mechanism for controlling movement because it does not require complex temporal and spatial coordination, greatly simplifying motor control.

Our model confirms that a stiffening wave caused by simultaneous and equal activations of the longitudinal and transverse muscles can push a bend along the arm. The stiffening wave straightens the model arm and generates kinematic features similar to those of natural movements (paper I, Fig. 7).

Purely feed-forward control?

The amplitude of the EMG signal at the beginning of the movement is positively correlated with the velocity of the bend point during the movement (Gutfreund et al. 1998), allowing prediction of the kinematic features of the movement from the EMG signal. This clearly indicates a strong feed-forward component in the control of the reaching movement.

Yet there is also some evidence for feedback-based components. In the octopus, the EMG wave front precedes the bend point by about 100 ms (Gutfreund et al. 1998), in contrast to the simulations where the bend point precedes the muscle activity (Fig. 3, paper I, Fig. 7). Part of the discrepancy may be explained by the excitation–contraction delay in the muscles, which was not included in the model. Assuming a 100-ms delay (based on a delay in fish muscles of the order of tens of milliseconds; Wardle 1975), the arm muscles would contract when the bend reaches that part of the arm. The remaining difference between the simulations and experimental results suggests that the primarily feed-forward propagation observed in the octopus may include some form of local feedback loops that sense the bend in the arm and adjust the propagating neuronal wave accordingly. Recently mechanoreceptors that could be part of such feedback loops were physiologically identified (unpublished data). It is reasonable that both components participate in shaping the octopus arm extension (see Gutfreund et al. 1998 for discussion). Adding a feedback component is thus a feasible extension of the model.

Working isometrically

We assumed that the longitudinal and the transverse muscles have the same functional properties (Matzner et al. 2000; Rokni and Hochner 2002) and that the muscle fibers are homogenously distributed throughout the arm. It is possible that the muscles are organized to maintain a balance of forces between them, which facilitates the antagonistic nature of their action. Using the proposed activation that stiffens the arm to control movement considerably simplifies the control task because there is no need for localized differential control. Furthermore, by working isometrically the muscles remain at the center of their working regime, readying the arm to perform other movements. If, as we suggest, the balance of forces between longitudinal and transverse muscles plays an important role in the arm's biomechanics, this may be demonstrated experimentally (e.g., by the ratio of cross-sectional areas of the different muscles).

Planning and control

What does the motor control system of the octopus plan to produce a reaching movement? Invariant description of movement is usually taken as evidence that the motor control system actually uses these variables to plan movement (Atkeson and Hollerbach 1985; Hollerbach and Flash 1982; Morasso 1981). In the extension movement, the bend point follows a simple planar path from the body center toward the target with a tangential velocity profile that is invariant across a variety of experimental conditions (Gutfreund et al. 1996). Therefore it would appear that the octopus motor system actively controls the position of the propagating bend (Gutfreund et al. 1996). However, our simulations show that a simple feed-forward strategy using a constant velocity wave of muscle activation produces a similar velocity profile that is also invariant across different wave velocities and muscle forces. Moreover, the experimental relation between integrated EMG and the bend's peak velocity described by Gutfreund et al. (1998) is also reproduced by the simulations (Fig. 7).

The velocity profile results from the interplay between the physical properties of the arm and the drag forces of water. Considering both the experimental and the simulation results, we can speculate that bend point position is not directly controlled but is, rather, the outcome of the following strategy when an octopus reaches toward a not too distant target:

1) Initiating a bend in the arm so that the suckers point outward.

2) Orienting the base of the arm in the direction of the target or just above it.

3) Propagating the bend along the arm at the desired speed by a wave of muscle activation that equally activates all muscles along the arm.

4) Terminating the reaching movement when the suckers touch the target by stopping the bend propagation and thus catching the target.

This strategy requires that the motor system set 4 parameters when initiating the reaching movement. The 2 angles for the orientation of the base of the arm and the speed with which the wave of muscle activation travels along the arm are the kinematic parameters. The force that the muscles create is the dynamic parameter that can be controlled through the level of muscle activation. The time it takes the arm to be straightened and reach a target is also an important kinematic aspect of the movement. This time depends on the speed of the wave of muscle activation and the force the muscles create.

This strategy has many advantages.

1) It considerably simplifies the task of planning and controlling the hyperredundant octopus arm: the inverse dynamics problem of the reaching movement (finding the muscle forces that cause the arm to reach toward a target) may be reduced to 2 relatively simple tasks: *i*) Determining the muscle activity that orients the base of the arm toward the target (not studied here). *ii*) Determining the muscle activity that stiffens the structure and pushes the bend forward with the desired velocity.

2) It uses the ability of the suckers all along the arm to catch objects, so that the grasp need not be so precise to be successful. It suffices that any part of the ventral side of the arm touches the target.

3) The arm movement minimizes the influence of water drag (see the discussion in paper I) and may also minimize the vortices and water currents created by the arm and reduce the chances of the octopus being noticed by potential prey.

The control parameters

The two control parameters in the model are analogous to the properties of the EMG signals: activation amplitude ac_a is partially analogous to the EMG amplitude and the activation traveling time ac_t can be easily transformed to propagation velocity $V = (arm\ length/ac_t)$, comparable to the propagation velocity of the EMG signal. Does the octopus really control these 2 parameters separately? Although, as yet, we have no experimental answer in the octopus, we used the model to separate the 2 variables and check the outcome of any combination of their values. Using the measure of arm straightness, we were able to show the relation between activation amplitude and activation traveling time, which results in the *minimum force curve* (Fig. 4). This *minimum force curve* may somehow be represented and used by the octopus motor system to set the minimal forces needed to follow a desired reaching trajectory.

Using forces larger than those dictated by the *minimum force curve* does not change the kinematics of the arm (Fig. 6), but produces a more stable reaching movement and greater resistance to perturbing forces (Fig. 9). This phenomenon appears similar to the cocontraction or coactivation phenomena of agonist and antagonist muscles in human and primate arms. Many activities require coordination of the muscles on both sides of a joint or muscle "cocontraction," which gives the joint stability and stiffness (Hogan 1984, 1985; Suzuki et al. 2001). However, we do not know whether the octopus actually uses this mechanism to deal with perturbing forces.

In conclusion, we have shown that a reaching movement can be achieved by controlling the activation traveling time ac_t and the activation amplitude ac_a, with no need to specifically control bend point position. This control scheme can be carried out solely by a simple feed-forward mechanism. However, we do not exclude feedback (especially local feedback loops) playing an important role in controlling and shaping arm movements. Our dynamic model of the octopus arm supports the hypothesis that the mechanism of the octopus extension movements is a wave of muscle stiffening that is propagated along the arm. It also confirms that this movement mechanism facilitates a dramatic reduction in the number of DOFs and thus the complexity of motor control of the octopus arm.

APPENDIX A

Here we show that, for the linear muscle model (presented in paper I), the relaxed shape of a rectangular segment has the minimal potential energy.

Let us consider the simple case of a rectangular segment. The 2 longitudinal muscles and 2 transverse muscles have the following force equation

$$f(t) = [k^0 + k^{\max} a(t)][l(t) - l_{rest}] + \alpha \frac{\mathrm{d}l(t)}{\mathrm{d}t}$$

We can neglect the damping coefficient α because we are considering only steady-state behavior. We assume that all muscles are equally activated and have the same stiffness. Thus we can collect the terms $[k^0 + k^{\max} a(t)]$ into a single stiffness value K

$$f(t) = K\,[l(t) - l_{rest}]$$

The potential energy stored in such a spring is

$$U = \tfrac{1}{2}K(l - l_{rest})^2$$

where l_{rest} is the muscle length at which the linear muscle model produces no force and its value is set to $0.4l_O^m$ (0.4 of the length at which the active muscle force peaks in the nonlinear muscle model, see paper I). The constant area of each segment is the same as its *relaxed area*, that is, the area of a segment when its 4 muscles are at their relaxed length. The relaxed length that was measured for the muscles was $0.8l_O^m$, so the area of each segment is $(0.8l_O^m)^2 = 0.64(l_O^m)^2$. The initial shape of the segment is an arbitrary rectangle with length b and width c. The segment's area is $S = bc$. The width and length of the relaxed shape are equal at $\sqrt{S}$ $(=0.8l_O^m)$.

The potential energy of the segment (neglecting the contribution of gravity and buoyancy) is the sum of the potential energy of its individual muscles

$$U_{seg} = 2 \cdot \tfrac{1}{2}K(b - l_{rest})^2 + 2 \cdot \tfrac{1}{2}K(c - l_{rest})^2$$

$$U_{seg} = K[(b - l_{rest})^2 + (c - l_{rest})^2]$$

Using the area, we express b as S/c and obtain

$$U_{seg} = K\left[\left(\frac{S}{c} - l_{rest}\right)^2 + (c - l_{rest})^2\right]$$

Plotting this function shows that there is a single minimum at $c = \sqrt{S}$. Let us check this point. To find the extremum point(s) we differentiate U_{seg}

$$\frac{dU_{seg}}{dc} = 2K\left(\frac{Sl_{rest}}{c^2} - \frac{S^2}{c^3} + c - l_{rest}\right)$$

and let the result equal zero

$$\frac{Sl_{rest}}{c^2} - \frac{S^2}{c^3} + c - l_{rest} = 0$$

For which the relaxed shape ($c = \sqrt{S}$) is a valid solution.

We differentiate U_{seg} twice to verify whether this is indeed a minimum point

$$\frac{d^2U_{seg}}{dc^2} = 2K\left(\frac{3S^2}{c^4} - \frac{2Sl_{rest}}{c^3} + 1\right)$$

Using the result ($c = \sqrt{S}$) and values of $l_{rest} = 0.4l_O^m$ and $S = (0.8l_O^m)^2$ we obtain

$$\frac{d^2U_{seg}}{dc^2} = 2K(3 - 1 + 1)$$

which is larger than zero and it is indeed a minimum.

The value of the minimal potential energy is

$$U_{seg} = 2K(\sqrt{S} - l_{rest})^2 = 2[k^0 + k^{\max}a(t)](\sqrt{S} - l_{rest})^2$$

Note that this value is changed by activation, but the fact that it is the minimal value does not depend on activation.

APPENDIX B

Here we generalize the above results to nonlinear muscles and segments with a general quadrilateral shape. The potential energy of the segment is the sum of the potential energies of its individual muscles. For the nonlinear muscles we do not have an explicit functional description of potential energy. We have used its definition to numerically integrate the muscle force

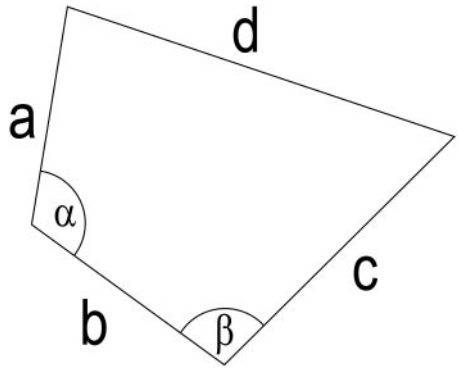

FIG. B1.

FIG. B1. A general quadrilateral can be described by 5 parameters; the length of 3 adjacent sides a, b, and c, and the 2 angles α and β. If the area is known, then the length of c can be expressed as a function of the other 4 parameters.

$$U(L, a) = \int_{L_{\min}}^{L} F(l, a)dl$$

where L is muscle length and a is the activation. The results for different activations a are shown in Fig. 1*B*. The shape of a general quadrilateral can be given by 5 parameters: the length of 3 adjacent sides and the 2 angles between those sides (Fig. B1). However, if the area of the quadrilateral is known, the length of the third side can be calculated based on that area. In other words, there is a 4-dimensional parameter space (the length of 2 adjacent sides and the 2 angles) that describes every general quadrilateral with the given area. We used a simple algorithm to search this space. The known area of the quadrilaterals was set to $S = (0.8l_O^m)^2$ and the lengths of the sides ranged from $0.1l_O^m$ to $2.5l_O^m$. The values for the two angles ranged from 0.1 to $\pi - 0.1$ radians. These values permit much larger shape changes than observed during the simulations. For each quadrilateral, we calculated the sum of the potential energies of its edges (according to the upper potential energy curve in Fig. 1*B*) and found that the quadrilateral with minimal potential energy is indeed a square.

ACKNOWLEDGMENTS

We thank Dr. Jenny Kien for suggestions and editorial assistance and G. Sumbre for help.

GRANTS

This work was supported by Defense Advanced Research Projects Agency Grant N66001-03-R-8043, by the Israel Science Foundation Grant 580/02, and by the Moross laboratory. T. Flash is an incumbent of the Dr. Hymie Moross Professorial Chair.

REFERENCES

Atkeson CG and Hollerbach JM. Kinematic features of unrestrained vertical movements. *J Neurosci* 5: 2318–2330, 1985.

Chirikjian GS and Burdick JW. A modal approach to hyper-redundant manipulator kinematics. *IEEE Trans Robot Autom* 10: 343–354, 1994.

Fiorito G, Planta CV, and Scotto P. Problem solving ability of *Octopus vulgaris* Lamarck (Mollusca, Cephalopoda). *Behav Neural Biol* 53: 217–230, 1990.

Gutfreund Y, Flash T, Fiorito G, and Hochner B. Patterns of arm muscle activation involved in octopus reaching movements. *J Neurosci* 18: 5976–5987, 1998.

Gutfreund Y, Flash T, Yarom Y, Fiorito G, Segev I, and Hochner B. Organization of octopus arm movements: a model system for studying the control of flexible arms. *J Neurosci* 16: 7297–7307, 1996.

Hogan N. Adaptive control of mechanical impedance by coactivation of antagonist muscles. *IEEE Trans Auto Cont* 29: 681–690, 1984.

Hogan N. The mechanics of multi-joint posture and movement control. *Biol Cybern* 52: 315–331, 1985.

Hollerbach JM. Fundamentals of motor behavior. In: *Visual Cognition and Action*, edited by Osherson, DN, Kosslyn, SM, and Hollerbach JM. Cambridge, MA: MIT Press, 1990, p. 151–182.

Hollerbach JM and Flash T. Dynamic interactions between limb segments during planar arm movement. *Biol Cybern* 44: 67–77, 1982.

Kier WM and Smith KK. Tongues, tentacles and trunks: the biomechanics of movement in muscular-hydrostats. *Zool J Linn Soc* 83: 307–324, 1985.

Matzner H, Gutfreund Y, and Hochner B. Neuromuscular system of the flexible arm of the octopus: physiological characterization. *J Neurophysiol* 83: 1315–1328, 2000.

Morasso P. Spatial control of arm movements. *Exp Brain Res* 42: 223–227, 1981.

Rokni D and Hochner B. Ionic currents underlying fast action potentials in the obliquely striated muscle cells of the octopus arm. *J Neurophysiol* 88: 3386–3397, 2002.

Sumbre G, Gutfreund Y, Fiorito G, Flash T, and Hochner B. Control of octopus arm extension by a peripheral motor program. *Science* 293: 1845–1848, 2001.

Suzuki M, Shiller DM, Gribble PL, and Ostry DJ. Relashionship between cocontraction, movement kinematics and phasic muscle activity in single joint arm movement. *Exp Brain Res* 140: 171–181, 2001.

Wardle CS. Limit of fish swimming speed. *Nature* 255: 727–729, 1975.

Wells MJ. *Octopus*. London: Chapman & Hall, 1978.

Wells MJ and Wells J. The function of the brain of octopus in tactile discrimination. *J Exp Biol* 34: 131–142, 1957.

Yekutieli Y, Sagiv-Zohar R, Aharonov R, Engel Y, Hochner B, and Flash T. Dynamic model of the octopus arm. I. Biomechanics of the octopus reaching movement. 94: 1443–1458, 2005.

Young JZ. The diameters of the fibres of the peripheral nerves of octopus. *Proc R Soc B Biol Sci* 162: 47–79, 1965.